Progress In Electromagnetics Research Letters, Vol. 102, 9–18, 2022

Capacitive-Wireless Power Transfer System for Power Supply of a Wireless Sensor System on a Propulsion Shaft

Van Ai Hoang and Young Chul Lee*

Abstract—We present a capacitive wireless power transfer (C-WPT) system using rotating capacitors for wireless sensor system (WSS) on propulsion shaft. In order to supply stable power to the WSS consisting of four sensors, a controller, and a radio module, we designed the rotating capacitor connected in parallel with multiple plates that minimizes the change in capacitance of the power coupling capacitor of the C-WPT system. A class-E converter and transformers topology are utilized to drive the C-WPT system for WSS. The fabricated C-WPT system transmitted stable power even when the rotational speed of the shaft was changed from 100 to 300 revolution per minute (rpm), and achieved power of 20.48 W and transmission efficiency of 64.29%.

1. INTRODUCTION

Recently, the maritime industry is once again at the cusp of a new era in automated ships, unmanned ships, and smart ships due to the growth of digitalization and innovation. The traditional conservative shipping industry is undergoing changes. All over the world, the smart ships are being equipped with the state-of-the art hardware and software technology that monitor and control the ship status and maintains its performance. A wireless sensor system (WSS) will be on the cusp of revolutionary changes with the emergence of innovative devices such as an internet of thing (IoT), wireless power transfer (WPT) technologies, and low-power and long-range radio modules.

Various sensors are installed on several parts of the ship to monitor its status and performance. Especially, a rotation per minute (RPM) meter, torque meter, and thrust meter are utilized for monitoring status of the rotating shaft. Recently, considering the WSS setup on the rotating shaft, the data and electric power need to be transferred between a rotor and stator. For example, slip rings and carbon brushes are traditionally connected to transfer signals and power across rotating devices [1]. However, they can cause failures due to the frictional rotation and physical connection problems. Therefore, they require frequent maintenance. In addition, another issue of the WSS on the shaft is the battery charge and its replacement; therefore, WPT can be a useful solution that satisfies these requirements for the WSS.

WPT technologies are developing rapidly and already used in many fields with a variety of applications such as wireless chargers [2, 3], medical devices, and robots [4, 5]. The WPT system has been found in two primary categories, inductive and capacitive WPTs (I-WPT and C-WPT, respectively). Considering applications on the rotating shaft, the I-WPT system with a rotary transformer is a promising alternative method of noncontact to replace the slip ring. However, the I-WPT has some limitations; the I-WPT cannot be used if metal objects exist between transmitting and receiving coils, and they will disturb the power transfer and possibly disrupt it completely, in which case a protected shield is required to prevent radiation of electromagnetic interference. In these issues, C-WPT system

Received 3 November 2021, Accepted 20 December 2021, Scheduled 29 December 2021
* Corresponding author: Young Chul Lee (rfleeyc@gmail.com).
The authors are with the Department of Marine Electronic, Communication and Computer Engineering, Mokpo National Maritime University, Mokpo, Republic of Korea.

can be an alternative, because C-WPT is utilized considering its inherent nature of electric field, and C-WPT has the ability to pass through any metal shielding environment. It is also simple to design and manufacture and allows more flexibility for the coupling plate design [6]. In particular, C-WPT is ideally suited for applications requiring contact-free over short distances. These properties make C-WPT more attractive for studies that require power transfer for wear mitigation rather than separation distances [7].

In general, C-WPT system can be categorized by power inverters and compensation networks. Several types of the inverter have been used on C-WPT system; these types include resonant push-pull inverters, power amplifiers (class D, class E, class EF, and class ϕ), and bridge inverters [8]. Compensation networks consist of series L, double-side LC, LCLC, CLLC compensations. The C-WPT system powered by a full-bridge inverter and rotary capacitors was developed in 2012 as an alternative to a slip ring or rotary transformer, and it provided 500 mA field current with an efficiency of 94% when the load rotated [9]. In 2014, a translational and rotating C-WPT system was built in a series resonant inductor and a full-bridge inverter combining a fluid bearing for general slip ring replacement applications [6]. Moreover, the rotational C-WPT system was tested with the circuits of the haft-bridge inverter and series L as sliding bearings that have been used for induction motor [10]. These cases required more complicated gate drivers because the way to build a bridge inverter needs to use two or four switches (gate driver ICs) and often leads to higher cost and lower reliability, especially for high frequency and high power applications. Although these studies have produced many interesting results, not much work has been reported to examine the different types of inverter topologies used in the field of rotary C-WPT area. In particular, the use of the class-E inverter with the compensation network for improving the system efficiency remains unexplored. Therefore, this inverter can be used as a suitable candidate for a rotary C-WPT system. Because this candidate only uses a single active switch and comprises fewer components, it is thus highly reliable. In commercial applications, class-E inverters are strongly recommended because they are reliable, efficient, cost-effective, and easy to control. However, the class-E operation of the converter is very sensitive to the variation of small capacitance of the coupling plate, and this small capacitance can degrade the power factor. Moreover, the condition of zero voltage switching (ZVS) at the resonant operation will be lost if the capacitance value is as small as the output capacitance of the main single switch. Meanwhile, a matching transformer scheme can be introduced to achieve ZVS condition as an effective driving way for C-WPT system with small capacitance.

The challenge in the C-WPT system is due to small coupling capacitance value. One solution is to connect an extra capacitor in parallel with the coupling capacitor. Therefore, multiple coupling plates are introduced here to increase the coupling coefficient value. Of course, as the diameter of the shaft increases, the size of the circular capacitor also increases, which may limit its application.

In this work, the C-WPT system using the rotating capacitors connected in parallel has been presented for WSS applications to the propulsion shaft. This system with the combined class-E converter and double-side transformer were used. The operation of the WSS on the rotating shaft was demonstrated.

2. THE DESIGN OF A C-WPT SYSTEM

2.1. The Design of the WSS System

Figure 1 shows a block diagram of the WSS with the C-WPT system to monitor the status of a propulsion shaft. There are two parts of the WSS, the receiver (Rx) and transmitter (Tx). The Tx part serves two purposes: sensing the status condition of the shaft and sending data to a PC. The components of the Tx part include four sensors, a controller, and a wireless communication (radio) module (XBEE Tx) that should be mounted on the rotating shaft. Sensors such as current, strain gauge, temperature, and pressure sensor are installed on the propulsion shaft. The current sensor of the Tx part is used to measure transferred power in operation. All obtained data were sent through the radio module and shown on the PC. The Rx part includes a power conversion circuit, a current sensor, a controller, and a radio module (XBEE Rx). The current sensor is used to measure the input power of the C-WPT system. Arduino is a central processing unit on both sides that processes the signals from sensors. The data of the Rx part were sent to the PC via USB connection. Power conversion converts DC power

supply into proper DC for sensors, controllers, and radio modules. In addition, the C-WPT includes stationary and rotary sides. At the stationary side, a primary auxiliary circuit is used to convert the electric power into a suitable form to excite stationary plates, which can generate the corresponding electric fields and transmit to the rotary side. At the rotary side, the rotary plates convert the electric fields back into electrical energy and supply it to the WSS though the secondary auxiliary circuit. The stationary and rotary plates have formed a rotating capacitor. This capacitor has functioned to transfer electrical power from stationary sources to moving loads.

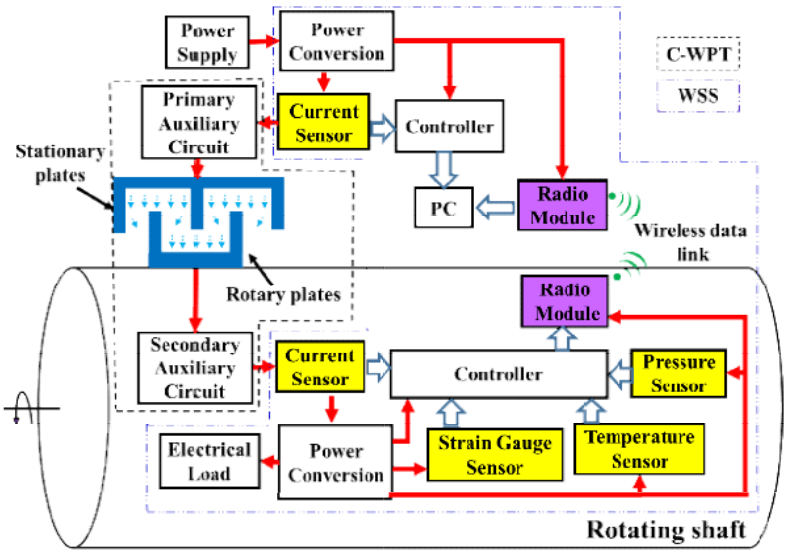

Figure 1. Block diagram of the WSS with a C-WPT system on the rotating shaft.

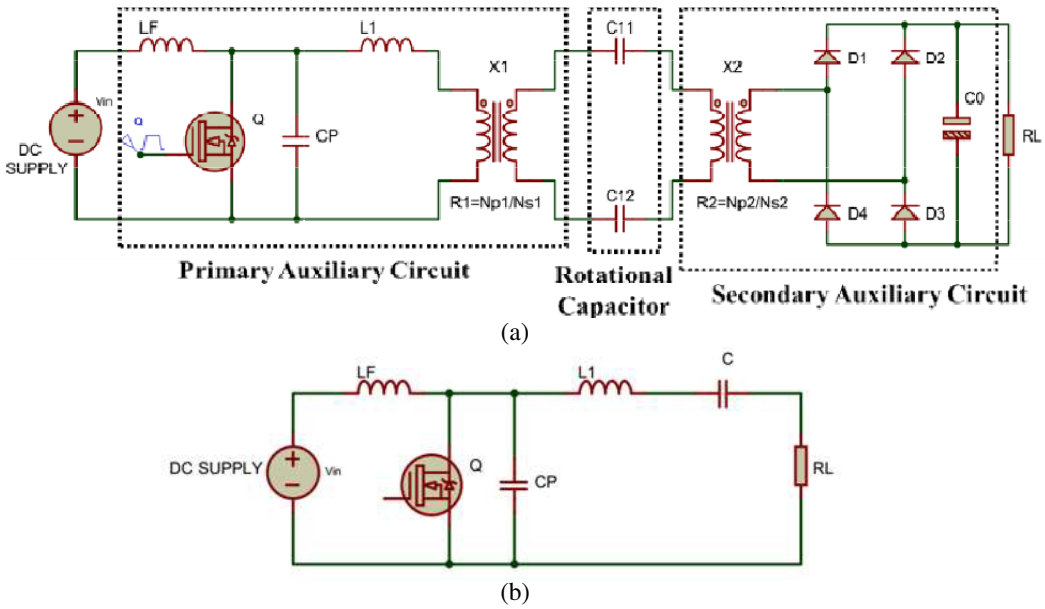

Figure 2. The circuit of the C-WPT system, (a) class-E power amplifier and transformers topology, (b) simpllified class-E.

2.2. A C-WPT Circuit

Figure 2(a) shows the circuit of the C-WPT system for power supply of the WSS on the rotating shaft. It consists of a primary auxiliary circuit, a rotational capacitor, and a secondary auxiliary circuit. The primary auxiliary circuit is the combination of a class-E power amplifier and a step-up transformer ($X1$). The class-E power amplifier converts the DC to high-frequency AC power and forms resonance with rotating capacitors. The step-up transformer makes the impedance of the coupling capacitance, to get wide zero voltage switching range and provide voltage gain to increase the voltages on the rotating plates. The secondary auxiliary circuit includes a step-down transformer ($X2$) and a rectifier. The step-down transformer increases the quality-factor and loses the fundamental limit. The rotational capacitors are capacitive coupling plates to transfer and receiver wireless power. The rectifier is used to convert the AC to DC power for a load. The whole circuit in Fig. 2(a) is then simplified as shown in Fig. 2(b). The general class-E power amplifier (PA) includes a choke inductor L_f, a MOSFET gate drive, and an inductor $L1$. The choke inductor L_f is assumed to be of great value so that the current crossing the load R_L is asinusoidal. The design was based on optimized conditions with the duty cycle D at 50%. For that, the circuit has designed the parameters according to References [11, 12]. The system parameters for the rotary C-WPT system are shown in Table 1.

Table 1. Parameters of the C-WPT circuit.

Parameter	**Value**	
Input voltage (V_{cc})	30	V
Frequency (f)	1	MHz
Quality factor (Q)	10	-
Load resistor (R_L)	50	Ω
Shunt Capacitor (C_P)	2.5	nF
Capacitor $C_{11} = C_{12}$	170	pF
Inductor (L_1)	18.37	μH
Choke inductor (L_f)	80.03	μH
Duty cycle (D)	50	%
Turn ratio $R_{TI} = n_1$	1 : 4	T/T
Turn ratio $R_{TI2} = n_2$	2.5 : 1	T/T

Figure 3 presents the simulation results of the proposed C-WPT system. The circuit was designed at 1 MHz operation frequency. In the case of the simulation in Fig. 3(a), the peak output voltage of the drain voltage of the MOSFET is approximately 86 V when the switch MOSFET is turned off, and it is lager than input voltage supply V_{cc} = 30 V with 2.8 times. During the turn-on state of the MOSFET, the voltage is not considerable around 4 V. Because the output voltage of the class-E amplifier is relatively high, this class-E amplifier can combine with the transformers as a method using high voltage to transfer wireless power. Considering the step-up transformer ($X1$), the designed ratio of the transformer $X1$ is 20 : 80. This means that the secondary voltage of the transformer $X1$ is 4 times greater than the primary voltage of the transformer $X1$. The output voltage of the primary auxiliary circuit is wireless transmission through the rotational capacitors and then will be reduced by the step-down transformer $X2$. The voltage ratio of the step-down transformer $X1$ = (primary voltage of the step-down transformer $X1$)/(secondary voltage of the step-down transformer $X1$) = 2.5. Fig. 3(b) shows the voltage of the load output without the rectifier, and the output voltage will increase with the increasing load condition, so that the output current of the load decreases as long as load voltage increases since the quality factor decreases. The average output voltage of the designed system is 34 V as shown in Fig. 3(c), and average current is 1 A. Following input power of the simulation circuit is 30 V × 1.2 A = 36 W.

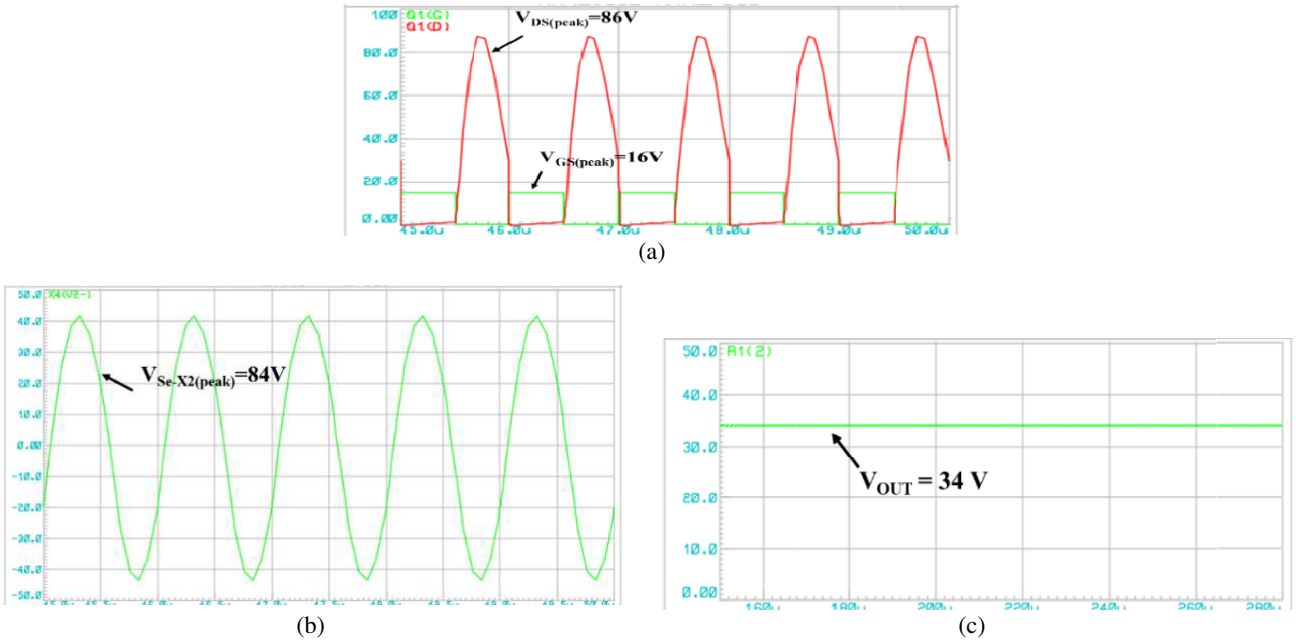

Figure 3. Simulation results: (a) waveforms of the class-E amplifier, (b) the secondary voltage of the step-down transformer, and (c) output voltage after the rectifier.

2.3. Multiple Coupling Plate for the Rotary C-WPT System

Figure 4 shows the designed and fabricated rotary capacitor that can operate as a capacitor without affecting the transmission power when the shaft rotates at a high speed. The rotary capacitor was

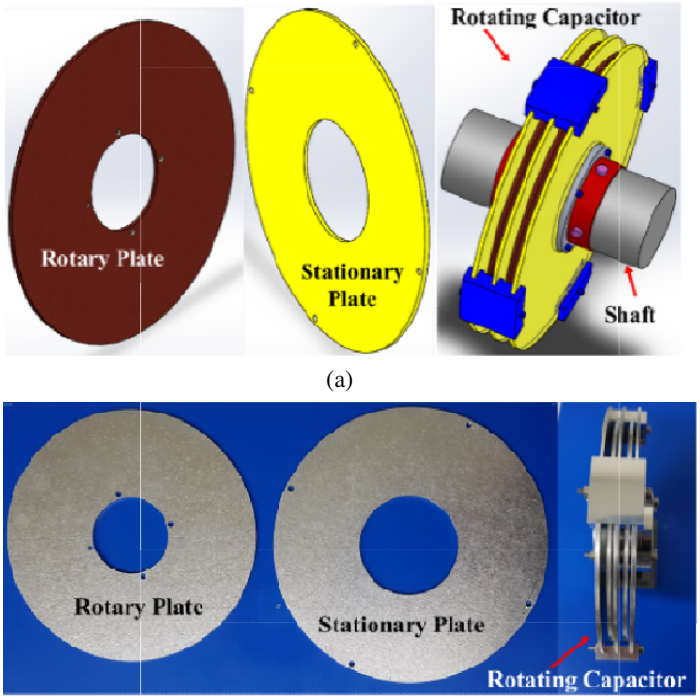

Figure 4. The (a) designed and (b) fabricated rotary capacitor.

split into two series capacitors with equal value, $C_{11} = C_{12}$. C_{11} and C_{12} are the forward and return capacitors, respectively. The purpose of multiple plates connected in parallel is to increase the value of the coupling capacitance. It can be convenient to use multiple plates of smaller value and size than a single plate with larger value and larger size. The rotary or stationary plates are connected to form the electrodes of the rotating capacitor [6].

The total capacitance of the coupling plates can be calculated using:

$$C = \varepsilon_r \varepsilon_0 \left(N_{Splates} - 1\right) \frac{A}{d} \tag{1}$$

where ε_r is the relativity dielectric constant of the material between the two conductive coupling plates ($= 1$ air). ε_0 is the permittivity of free space ($8.854 \times 10^{-12}\,\mathrm{Fm}^{-1}$). A is the overlapping area of the two plates. $N_{Splates}$ is the number of stationary plates. d is the gap between the plates.

Aluminum plates were used for the circle plate capacitors due to their simplicity, lightness, and low cost. The thickness of all aluminum plates is the same and does not affect the coupling capacitance. Stationary and rotary plates are separated by an air gap of 1–5 mm. The capacitances for both forward and return are equal, $C_{11} = C_{12} = 170\,\mathrm{pF}$. Thus, C_{11} and C_{12} can be combined into a single capacitor for convenience, and the total capacitive interface $C_1 = C_{11}//C_{12} = 170/2 = 85\,\mathrm{pF}$. The diameter of the propulsion shaft is 4 cm. The inner and outer radii of the rotary plates are 2 cm and 6.85 cm, respectively. The stationary plates have the inner radius of 2.7 cm and outer radius of 7.5 cm. Parasitic inductance may occur due to large area aluminum plates and their connection. However, at the low frequency of 1 MHz, the value is small, and the effect is negligible. In Fig. 5, results of the simulated and measured capacitances of the rotating capacitor are presented, and the two values agree well.

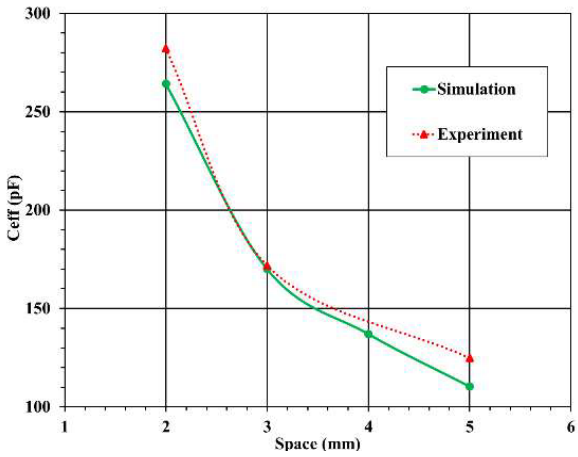

Figure 5. The simulated and measured capacitance of the rotating capacitor.

3. SET UP C-WPT SYSTEM AND MEASURED RESULT

3.1. Fabricated C-WPT System

To evaluate the performance of the C-WPT system using the rotating capacitor, the C-WPT system on the small test shaft which consists of the class-E converter, two transformers, and two rotating capacitors has been installed as shown in Fig. 6. The WSS includes sensors, wireless communication modules, and controllers, which is also presented in Fig. 6. Several components on the shaft can affect the motion of the high-speed rotating shaft. Therefore, this issue should be considered in the final system. The experimental C-WPT system was set up with discrete components. The class-E converter and step-up transformer are connected to the stationary plates of the two rotating capacitors 1 and 2. The rotary plates are linked to the step-down transformer, rectifier, and WSS. All data of the WSS on the shaft are sent to the external PC via wireless communication modules (Zigbee). There is a rotating shaft connected to the motor to simulate the rotation speed by controlling the speed adjustment

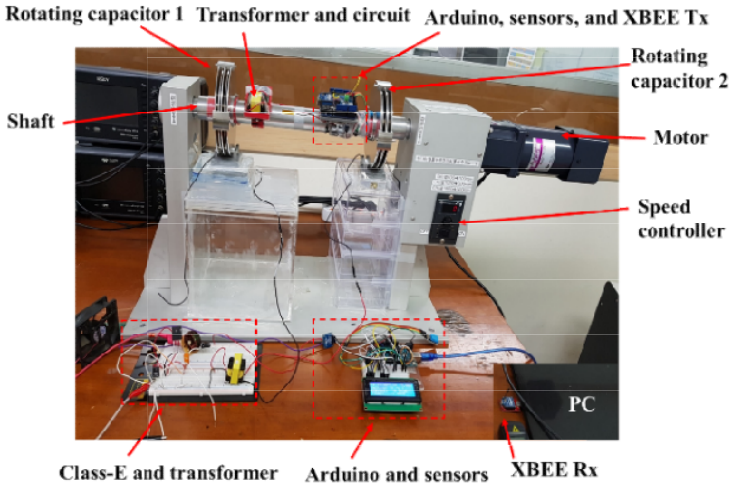

Figure 6. Experiment setup for WPT system on a small scale test shaft.

knob. Theoretically, the peak switch voltage is about 2.8 times the value of DC power supply, V_{cc}. In this case, V_{ds} (max) approximately equals 86 V. This means that the transistor breakdown voltage in MOSFET must be sized accordingly. Therefore, a high-speed power MOSFET (IRF510) [13] was utilized as the inverter switching device. It was selected because of its high V_{DS} and its current rating which is sufficient to support the experimental work, with values of 100 V and 5.6 A, respectively. The datasheet [14] shows that the MOSFET's parasitic output capacitance has a value of 81 pF at 25 V. This is considered very low and is thus easy to achieve under soft-switching conditions. For the full-bridge rectifier circuit at the rotary side, power Schottky rectifier diodes (STPS5L40) were chosen to serve as a rectifier. As there is extremely low forward voltage, power loss can be minimized at the rectifier side. Commercial Generator (DFG-8005) [15] was utilized to generate the inverter's PWM signal. It is so, as it is convenient to fine-tune the duty cycle (D) and the switching frequency (f).

3.2. Experiment Results

Figure 7 shows the experimental result for the C-WPT system. As shown in Fig. 7(a), the experiment peak voltage across the drain gate of the MOSFET during the turn-of time was 85.6 V. The switching control signal was used to control the gate (G) of the MOSFET, which is originally 16 V with frequency 1 MHz at 50% duty cycle. During the turn-on time, the peak voltage of the drain is 4.5 V and the same with simulation. The output voltage of the class-E amplifier is supplied to the primary side of the step-up transformer $X1$. The step-up transformer $X1$ operates on the way for increasing alternating voltage according to the original design ratio. These output voltage and current have been supplied for two stationary plates. At the time, wireless power transmission is made between rotary and stationary plates.

The voltage between the two polarities of the rotary plates is also the input voltage of the primary winding of the step-down transformer $X2$. The secondary winding voltage of the $X2$ or output voltage before rectifier is shown in Fig. 7(b). The peak-to-peak voltage of the secondary winding of the transformer $X2$ was 70 V. The experimental voltages of the transformers $X1$ and $X2$ are lower than the values of simulation results. Because designed transformers were traditionally isolation transformers, pulse transformers are need to use in terms of input transmitting electrical pulses and high operating frequency. The output voltage is finally rectified via the rectifier (diode bridge). The average voltage is about 22.4 V as shown in Fig. 7(c). The output voltage is relatively stable when the filter capacitor is added before the loading resistor.

The input power of the class-E converter is $30 \times 1.05A = 31.5$ W. The output power of the C-WPT system is $22.4 \times 0.9 = 20.16$ W, resulting in the efficiency of 64%, operated at 1 MHz switching frequency and 50 Ω load. Fig. 8 shows details about the performance of the system when the load changes. It can be seen that the efficiency of the C-WPT system increases with increase of the power. Efficiency also

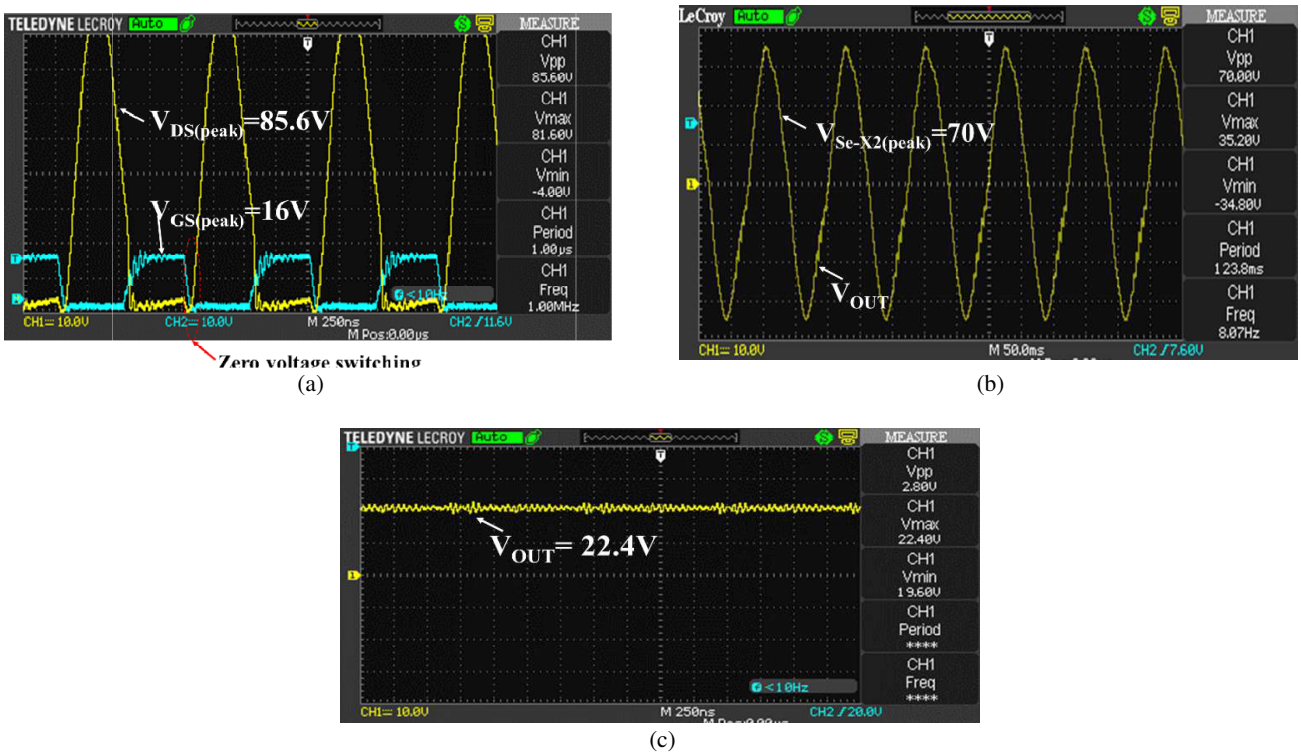

Figure 7. Experimental results: (a) waveforms of the class-E amplifier, (b) the secondary voltage of the step-down transformer, and (c) output voltage after the rectifier.

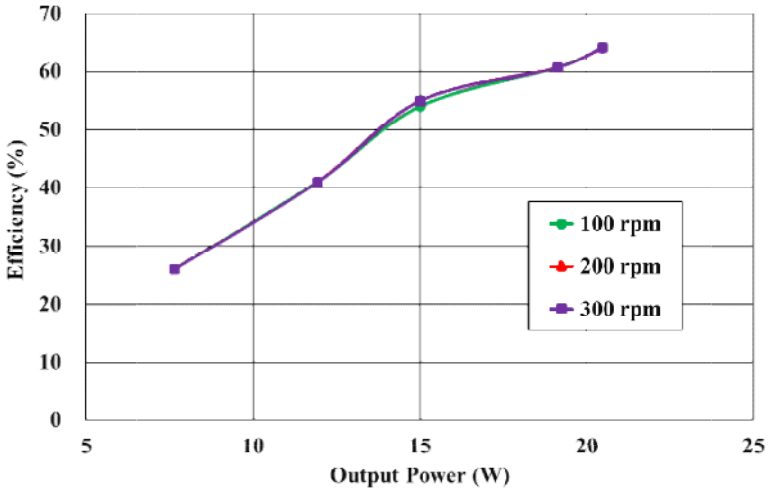

Figure 8. Efficiency of the C-WPT system.

depends on the change of the load value. The principle of the maximum power transfer results from a matching between the source and load impedances regardless of the system structure. The variation of the energy efficiency and output power is as a function of the ratio of RL (load resistance) and RS (source resistance). For the fixed RS, the output power will be maximum when RS equals RL. For RL is higher than RS, the energy efficiency becomes higher when RL becomes higher.

4. CONCLUSIONS

In this work, the C-WPT using rotating capacitors for supplying stable power to the WSS on the rotating shaft was designed and fabricated, and its characteristics were presented. To minimize the capacitance change of the fabricated rotating capacitors, the capacitors were designed in which multi-stationary and rotary plates were connected to the fixture and the rotating shaft, respectively. The designed capacitance of 170 pF was well matched to the fabricated one. The class-E converter and transformers of the C-WPT prototype were designed and implemented to demonstrate efficient WPT across the rotating load. The measured voltages of the transformers, are lower than the simulation results, due to real and lossy transformers. An output power of 20.48 W and a power transfer efficiency of 64.29% were achieved at 1 MHz operating frequency. The performance of the fabricated C-WPT prototype proved that the WSS on the shaft could be stably driven.

ACKNOWLEDGMENT

This work was supported by Basic Science Research Program through the National Research Foundation of Korea (NRF) funded by the Ministry of Education (2017R1D1A3B03036543).

REFERENCES

1. Hall, R. D. and R. P. Roberge, "Carbon brush performance on slip rings," *Conference Record of 2010 Annual Pulp & Paper Industry Technical Conference*, 1–6, June 2010.
2. Da Silva, G. G. and C. A. Petry, "Capacitive wireless power transfer system applied to low-power mobile device charging," *International Journal of Electrical Energy*, Vol. 3, No. 4, 230–234, December 2015.
3. Tran, D. H., V. B. Vu, and W. Choi, "Design of a high-efficiency wireless power transfer system with intermediate coils for the on-board chargers of electric vehicles," *IEEE Transactions on Power Electronics*, Vol. 33, No. 1, 175–187, January 2018.
4. Campi, T., S. Cruciani, M. Feliziani, and A. Hirata, "Wireless power transfer system applied to an active implantable medical device," *2014 IEEE Wireless Power Transfer Conference*, 134–137, 2014.
5. Narayanamoorthi, R., A. Vimala Juliet, C. Bharatiraja, P. Sanjeevikumar, and Z. M. Leonowicz, "Class E power amplifier design and optimization for the capacitive coupled wireless power transfer system in biomedical implants," *Energies*, Vol. 10, No. 9, 1409, September 2017.
6. Ludois, D. C., M. J. Erickson, and J. K. Reed, "Aerodynamic fluid bearings for translational and rotating capacitors in noncontact capacitive power transfer systems," *IEEE Trans. Ind. Appl.*, Vol. 50, No. 2, 1025–1033, 2014.
7. Dai, J. and D. C. Ludois, "Single active switch power electronics for kilowatt scale capacitive power transfer," *IEEE J. Emerg. Sel. Top. Power Electron.*, Vol. 3, No. 1, 315–323, 2015.
8. Lu, F., H. Zhang, and C. Mi, "A review on the recent development of capacitive wireless power transfer technology," *Energies*, Vol. 10, No. 11, 1752, November 2017.
9. Ludois, D. C., J. K. Reed, and K. Hanson, "Capacitive power transfer for rotor field current in synchronous machines," *IEEE Transactions on Power Electronics*, Vol. 27, No. 11, 4638–4645, 2012.
10. Hagen, S., R. Knippel, J. Dai, and D. C. Ludois, "Capacitive coupling through a hydrodynamic journal bearing power rotating electrical loads without contact," *2015 IEEE Wireless Power Transfer Conference (WPTC)*, 1–4, 2015.
11. Yusop, Y., M. S. Md. Saat, S. H. Husin, S. K. Nguang, and I. Hindustan, "Performance assessment of class-E inverter for capacitive power transfer system," *COMPEL — The International Journal for Computation and Mathematics in Electrical and Electronic Engineering*, Vol. 36, No. 4, 1237–1256, 2017.

12. Choi, S. and H. Choi, "Capacitive wireless power transfer system with double matching transformers for reduced stress and extended ZVS range," *2015 IEEE International Telecommunications Energy Conference (INTELEC)*, 1–6, 2015.
13. Power MOSFET, www.infineon.com/cms/en/product/power/mosfet/.
14. IRF510S, SiHF510S Power MOSFET, https://www.vishay.com/doc?91016.
15. DFG-8005 5 MHz DDS, https://www.testermart.com/data/datadb/FLIR/DFG-8010,8020%20series_KR.pdf.